g factor of the exotic N=21 isotope 34A l: probing the N=20 and N=28 shell gaps at the border of the "island of inversion"

P. Himpe, G. Neyens, D.L. Balabanski, G. Bélier, J.M. Daugas, Francois de Oliveira Santos, M. de Rydt, K.T. Flanagan, I. Matea, Pierre Morel, et al.

g factor of the exotic N=21 isotope ^{34}Al: probing the $N = 20$ and $N = 28$ shell gaps at the border of the "island of inversion".

P. Himpe [a], G. Neyens [a,1], D.L. Balabanski [b], G. Bélier [c],
J.M. Daugas [c], F. de Oliveira Santos [d], M. De Rydt [a],
K.T. Flanagan [a], I. Matea [e], P. Morel [c], Yu. E. Penionzhkevich [f],
L. Perrot [d], N.A. Smirnova [g,2], C. Stodel [d], J.C. Thomas [d],
N. Vermeulen [a], D.T. Yordanov [a], Y. Utsuno [h], T. Otsuka [i]

[a]*K.U. Leuven, Instituut voor Kern- en Stralingsfysica, B-3001 Leuven, Belgium*

[b]*INRNE, Bulgarian Academy of Sciences, BG-1784 Sofia, Bulgaria*

[c]*CEA/DIF/DPTA/PN, BP 12, F-91680 Bruyeres le Chatel, France*

[d]*GANIL, BP 55027, F-14076 Caen Cedex 5, France*

[e]*Centre d'Etudes Nuclaires de Bordeaux Gradignan - CENBG, F-33175 Gradignan, France*

[f]*Joint Institute for Nuclear Research, FLNR, Dubna 141980 Moscow Region, Russia*

[g]*Universiteit Gent, Vakgroep Subatomaire en Stralingsfysica, B-9000 Gent, Belgium*

[h]*Japan Atomic Energy Agency, Tokai, Ibaraki 319-1195, Japan*

[i]*Department of Physics and Center for Nuclear Study, University of Tokyo, Hongo, Tokyo 113-0033, Japan
and RIKEN, Hirosawa, Wako-shi, Saitama 351-0198, Japan.*

Abstract

For the first time the g factor of an isotope beyond $N = 20$ near the 'island of inversion' has been measured. A ^{34}Al radioactive beam was produced in a one-neutron pickup reaction on a ^{36}S primary beam at 77.5 MeV/u, providing a large spin-polarization for application of the β-Nuclear Magnetic Resonance (β-NMR) method. The measured g factor of ^{34}Al, |g|=0.539(2), combined with results from earlier β-decay studies, allows to firmly assign a ground state spin/parity 4^-. Comparison to large scale shell model calculations reveals that a dominant amount of intruder components is needed in the ^{34}Al wave function to account for the observed large magnetic moment $\mu = (+)2.156(16)\mu_N$. This reveals $Z = 13$ to be a true 'transition number' between the normal $Z = 14$ Si isotopes and the abnormal $Z = 12$ Mg isotopes. The sensitivity of this odd-odd ground state dipole moment to

the $N = 20$, as well as the $N = 28$ gap, reveals that both are significantly reduced, despite $Z = 13$ being outside the conventional island of inversion.

The disappearance of magic numbers is one of the amazing features discovered in the physics of nuclei far from stability. A good example is the $N \sim 20$ region, where a mass anomaly in ^{31,32}Na [1] and a large deformation observed for $^{32}_{12}$Mg [2] were in contrast to the spherical behavior expected for a nucleus with magic number $N = 20$. The unusual properties of these nuclei were explained in terms of states with two neutrons excited across the $N = 20$ shell gap, called $2p2h$ (2 particle - 2 hole) intruder states. The region where such intruder state is the ground state, is often referred to as the "island of inversion", and it was predicted [3] to consist of nine nuclei with $10 \leq Z \leq 12$ and $20 \leq N \leq 22$. Experiments have shown however, that some isotopes with $N < 20$ also belong to the island of inversion, e.g. the $N = 19$ isotones $^{30}_{11}$Na and $^{31}_{12}$Mg [4,5]. This might be explained by a decrease of the $N = 20$ shell gap [6,7] for isotopes below $Z = 14$, because of the strong $T = 0$ monopole interaction between neutrons in the $0d_{3/2}$ and protons in the $0d_{5/2}$ orbits [8,9]. On the other hand, little experimental data are available for nuclei with $N > 20$ and even none for $N = 21$ isotopes with $Z < 14$. The odd-odd $N = 21$ isotopes are particularly sensitive to the proton-neutron part of the shell model interactions. Recently developed effective shell model interactions, used to describe properties in this mass region, differ mainly in this part and thus experimental observables that probe this part of the effective interactions are crucial inputs to test their validity.

As a function of proton number, not much is known either on how far the island is extending beyond $Z > 12$. Since the $_{14}$Si isotope is known to have a normal ground state [10], the ground state structure of the transitional $_{13}$Al isotopes is of great interest. A recent measurement of the magnetic moments of Al isotopes up to ^{33}Al ($N = 20$) suggested a sizable amount ($> 25\%$) of intruder mixing into the ^{33}Al ground state [11]. Such mixing was not observed through the ^{33}Al β-decay [12].

In this Letter we aim to further investigate whether intruder configurations contribute to the neutron rich Al ground state wave functions, in which case another modification of the concept of 'island of inversion' has to be considered, now towards higher Z. For the first time, the ground state structure of an isotope with 21 neutrons close to the originally proposed 'island of inversion', can be investigated by measuring its g factor (related to the magnetic moment $\mu = Ig\mu_N$). The magnetic moment is a decisive observable to determine which

---

[1] corresponding author: Gerda Neyens, e-mail: gerda.neyens@fys.kuleuven.be
[2] Present address: Centre d'Etudes Nuclaires de Bordeaux Gradignan - CENBG, UMR 5797 CNRS/IN2P3 Univ Bordeaux 1, F-33175 GRADIGNAN, FRANCE.

configuration dominates the ground state. E.g. in the $N = 19$ isotones ^{30}Na and ^{31}Mg the magnetic moment played a key role in determining that their ground state has a nearly pure intruder $2p2h$ configuration, and thus they occur inside the island of inversion [4,5,8]. Furthermore, the moments of odd-odd isotopes are shown to be also sensitive to odd-proton odd-neutron configuration mixing, as demonstrated e.g. for ^{30}Na [8]. Therefore, the magnetic moment of ^{34}Al will not only be sensitive to mixing of intruder configurations in its wave function (and thus to the strength of the $N = 20$ gap), but also to configuration mixing between the $\pi(sd)\nu 0f_{7/2}$ and the $\pi(sd)\nu 1p_{3/2}$ configurations (and thus to the $N = 28$ gap between the $\nu 0f_{7/2}$ and $\nu 1p_{3/2}$ orbits). This $N = 28$ gap is known to vary from 2 MeV in $^{40}_{20}$Ca down to 1 MeV in $^{35}_{14}$Si [13,14], but no experimental information is available for lower Z values. Through the magnetic moment of the $N = 21$ isotope ^{34}Al, we can now for the first time probe the interaction between sd protons and fp neutrons, for isotopes with an open $\pi 0d_{5/2}$ orbit, thus approaching the island of inversion. By evaluating the amount of intruder mixing in the Al ground states through a consistent comparison of their moments with large scale shell model calculations, one can see how the gradual transition from normal Si to deformed Mg isotopes, suggested by the ^{33}Al g factor analysis [11], occurs for $N = 21$. This will reveal whether or not intruder states become more important in $N = 21$ than in $N = 20$ isotopes, which was never verified experimentally. This result will thus for the first time shed light on the island of inversion beyond $N = 20$ and possibly extend the island towards higher Z values.

The ^{34}Al half life, $t_{1/2}$=56.3(5) ms [13], is ideally suited for application of the β-Nuclear Magnetic Resonance (β-NMR) technique [15], for which a spin-polarized ^{34}Al beam is required. In our earlier studies, spin-polarized Al beams have been produced through the fragmentation of a ^{36}S primary beam at 77 MeV/u [11,16] by selecting fragments in the wing of their longitudinal momentum yield curve. To produce ^{34}Al (N=21) fragments from a primary ^{36}S (N=20) beam, the ions have to pick-up one neutron from the target and three protons should be released. The spin-polarization process in a pure pick-up reaction was investigated by Groh et al. who demonstrated that ^{37}K fragments produced by a one-proton pick-up from a ^{36}Ar beam at 150 MeV/u, are spin-polarized and the largest polarization was observed for fragments selected in the center of the longitudinal momentum distribution [17]. For ^{34}Al fragments produced in the reaction of a ^{36}S^{16+} beam (77.5 MeV/u) on a ^{9}Be target ($\sim$200 mg/cm^2) Turzo et al. [18] also observed the largest polarization at the maximum of the longitudinal momentum yield curve. The observed trend of the polarization as a function of the fragments momentum could be reproduced using the pick-up model suggested by Groh et al. [17] and assuming that the subsequent loss of protons does not modify the polarization. The experimental procedure has been extensively described in [18] and was used in this work. With the LISE fragment separator at GANIL [19] a polarized ^{34}Al beam with purity 93% and a rate of 900 pps (for a primary beam intensity of typically
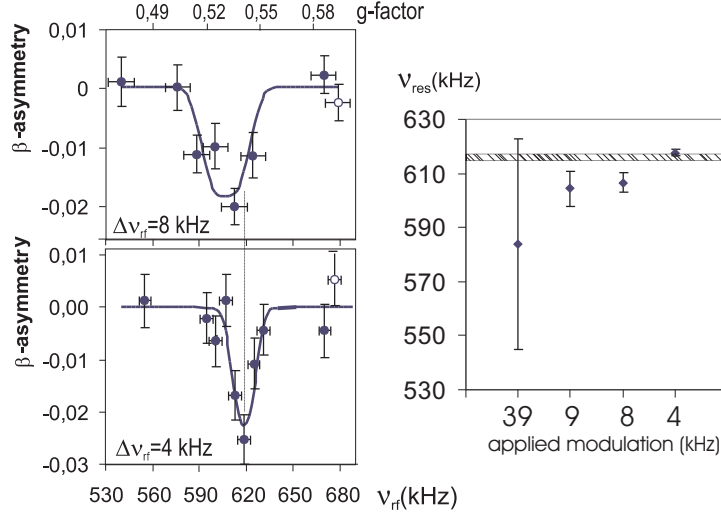
Fig. 1. NMR resonances of ^{34}Al in Si crystal. The open dots are obtained with the rf-field switched off. The right panel shows the results from individual scans with their weighted mean.

2eμA) was selected. The beam has been implanted in a Si crystal at room temperature, which was immersed into a static magnetic field applied parallel to the polarization symmetry axis. The polarized ensemble decays asymmetrically along the polarization axis, which is observed as an asymmetry in the count rate in two detectors placed parallel (N(0°)) and antiparallel (N(180°)) to the field direction. The g factor is determined by measuring a destruction of the spin-polarization as a function of an applied radio-frequency (rf) field with frequency ν_{rf}. Typically five to ten discrete rf-frequencies are applied during a few seconds each, after which the rf-field is switched off for a few seconds. Such a scan is repeated until the statistical error on the asymmetry at resonance is at least 3σ out of the baseline. Every applied frequency is modulated over a range $\Delta\nu_{rf}$ in order to guarantee that the resonance condition is fulfilled in at least one of the applied frequency ranges and that full destruction of the initial polarization occurs. When the applied rf range $\nu_{rf} \pm \Delta\nu_{rf}$ covers the Larmor frequency $\nu_L = \frac{g\mu_N B_0}{h}$, the polarization is destroyed and this is observed as a change in the β-asymmetry $= \frac{N(0°)}{N(180°)} - 1$. More details on the experimental β-NMR set-up and methodology can be found in [11].

A search for a resonance signal in the β-decay asymmetry was performed for a large g factor range, from $g = 0.22$ up to $g = 0.85$, using a large frequency modulation of 20 kHz. A change in asymmetry was observed for $g = 0.51\pm0.03$. In order to obtain the g factor more precisely, three measurements with a smaller frequency modulation of 9 kHz, 8 kHz and 4 kHz were performed. The observed resonance curves for the latter two are shown in Figure 1, where the β-asymmetry is normalized to the average of the outermost data points which are out of resonance. The resonances are fitted to a theoretical curve that is calculated by numerically integrating the coupled differential equations

4

describing the interaction of the nuclear spins with a frequency-modulated rf-field [11,20]. This curve is convoluted with a Gaussian in order to account for the inhomogeneous line broadening due to the fact that the magnetic field is not very homogeneous across the beam spot ($\Delta B \approx 0.4\%$). A χ^2 minimization procedure is used with ν_{rf}, the rf-field strength and the amount of asymmetry A as free parameters. A consistent result is obtained with A=2.0(4)% and $B_{rf} = 0.3$ mT. The weighted mean of these results is presented in Fig. 1 by the dashed bar, leading to $|g| = 0.539(1)$. Because the scattering on the data is larger than the statistical errors, we adopt the standard deviation as the final error, resulting in $|g(^{34}\text{Al})| = 0.539(4)$.

The normal ground state configuration of ^{34}Al is dominated by a $\pi d_{5/2}^{-1} \nu f_{7/2}$ configuration with respect to a ^{34}Si core [21], allowing possible spins $(1, ..., 6)^-$. Mixing with $2p2h$ neutron excitations provides similar spin possibilities. The $1p1h$ intruder configuration $\pi d_{5/2}^{-1} \nu(d_{3/2}^{-1} f_{7/2}^2)$ leads to $(1, ..., 4)^+$ spin/parities. According to Paar's parabolic rule [22], ground state candidates are then $3^-, 4^-, 5^-$ or $1^+, 4^+$. As no feeding to the 0^+ ground state of ^{34}Si is observed in the ^{34}Al β-decay [21], a 1^+ intruder ground state is excluded. The 4255 keV level in ^{34}Si decays within less than 300 ns to its 0^+ ground state and therefore this level must have a spin lower than 4 [13]. Because this level is populated with large intensity in the ^{34}Al β-decay, spin 5 has been excluded as ground state spin [13]. Our measured g factor, $|g_{exp}| = 0.539(2)$, allows to firmly exclude also the 3^- and 4^+ options. With the additivity rule for nuclear moments [15] the Schmidt values are: $g_{sch}(\pi d_{5/2}^{-1} \nu d_{3/2}^{-1}, 4^+) = +1.49$ and $g_{sch}(\pi d_{5/2}^{-1} \nu f_{7/2}, 3^-) = -0.03$. A more reliable estimate is obtained using empirical single particle g factors, as deduced from normal neighboring isotopes, g(^{31}Al, $5/2^+$) $= +1.532(2)$ [11] and g(^{35}Si, $7/2^-$) $= -0.468(1)$ [23], leading to $g_{emp}(4^+) = +1.26$ and $g_{emp}(3^-) = -0.05$. All values strongly deviate from our observed g factor and thus we can firmly exclude 3^- and 4^+ as ground state spin assignments. The empirical g factors for the 4^- and 5^- configurations are rather similar, $g_{emp}(5^-) = +0.34$ and $g_{emp}(4^-) = +0.21$, and therefore the 5^- assignment can not be excluded by this g factor measurement. However, the spin 5 was excluded from the β-decay study [13]. Thus the $I^\pi = 4^-$ assignment remains the only one that is compatible with both the decay and the g factor data.

We compare our measured g factor to advanced large scale shell model calculations. Because the shell model calculates magnetic moments and not g factors, we compare the deduced experimental magnetic moment assuming spin 4 or spin 5 (Table 1), to the values that are predicted for the 4^- and 5^- states. With all shell model interactions, these two states are competing to be the ground state: they occur both below 100 keV. The large-scale shell model calculations have been performed using two commonly used effective shell model interactions: the sdpf interaction developed by the Strasbourg-Madrid group [24] and the SDPF-M interaction developed by the Tokyo group [6]. Both interactions

start from the USD interaction [25] for the sd shell, while different cross-shell interactions are used. Also their monopole matrix elements have been tuned differently, leading to other effective single particle energies and shell gaps. The major differences are summarized by Caurier et al., and illustrated in Fig. 1 of [14]. The sdpf interaction was modified in order to reproduce the low energy of the $3/2^-$ level in ^{35}Si, which is dominated by the $\nu p_{3/2}$ configuration [13]. Thus the $N = 28$ gap in this new sdpf.sm is smaller than in SDPF-M, and for odd-odd isotopes with 21 neutrons it predicts a larger mixing with configurations involving the $\nu 1 p_{3/2}$ orbit, which leads to a larger magnetic moment. On the other hand, the $N = 20$ shell gap is smaller in the SDPF-M interaction, which invokes a larger contribution of intruder configurations in the ground state wave functions and yet the appearance of a larger 'island of inversion', including the ^{33,34}Al isotopes. As the nuclear moments of odd-odd $N = 21$ isotones are thus very sensitive to these two shell gaps, comparing their experimental values to the predictions from both large-scale calculations provides a crucial test for these effective shell model interactions. The present result is the first that is experimentally accessible for such a comparison.

In both calculations a ^{16}O core is used, with 5 protons in the sd shell. In the sdpf.sm calculations we allowed up to 3 neutron excitations from the sd to the $\nu(0f_{7/2}1p_{3/2})$ orbits, while in the SDPF-M calculations no limitation on the number of excitations across $N = 20$ is considered. Thus mixing between normal and intruder configurations (up to $2p2h$ in sdpf.sm and up to $npnh$ in SDPF-M) is included in both calculations. Free-nucleon g factors have been used, as in our earlier studies on the Al and Mg isotopes [5,11]. The results from both shell model calculations are compared to the experimental magnetic moments in Table 1 (SDPF-M' is discussed further).

Borremans et al. [28] have shown that the structure of the odd Al isotopes up to $A = 31$ is dominated by a proton hole in the $\pi d_{5/2}$ orbital, and that their magnetic moments are well described with the USD interaction with protons and neutrons restricted to the sd shell [25]. From stable ^{25}Al up to $N = 18$ ^{31}Al, the magnetic moments are reproduced to better than 2%. For the $N = 20$ isotope ^{33}Al, Himpe et al. [11] reported recently a deviation of 4% from the USD-value. Considering the high experimental precision that is obtained for all moments and the good agreement with the USD predictions for the less exotic isotopes, they concluded that this deviation is an indication for a $2p2h$ intruder state admixture into the ^{33}Al ground state wave function. Indeed, by including excitation across the $N = 20$ shell gap, the calculated moment decreases from $4.26\mu_N$ (without $2p2h$ contribution) towards respectively $4.22\mu_N$ with sdpf.sm (with 10% $2p2h$ contribution) and $3.84\mu_N$ with SDPF-M (with 59% $2p2h$). As the experimental magnetic moment of $4.01\mu_N$ lies between the latter two values, it was concluded that some intruder state admixture into the ^{33}Al

Table 1

Magnetic moments of Al isotopes (data from [26], [11] and this work). The absolute deviation between theory and experiment is given in brackets.

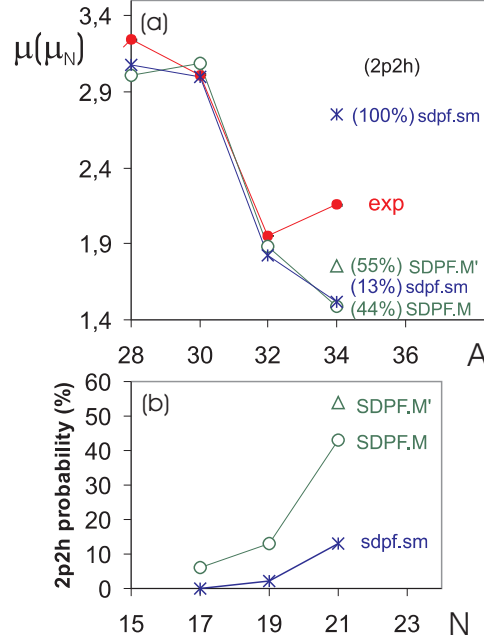| A	N	I^π	$t_{1/2}$	μ_{exp}	$\mu_{sdpf.sm}$	μ_{SDPF-M}	$\mu_{SDPF-M'}$
Odd-even							
33	20	$5/2^+$	44 ms	4.088(5)	4.22 (3.2%)	3.84 (6.0%)	3.83 (6.3%)
31	18	$5/2^+$	640 ms	3.830(5)	3.81 (0.5%)	3.77 (1.5%)	3.76 (1.8%)
Odd-odd							
34	21	4^-	56 ms	2.156(16)	1.52 (29%)	1.49 (31%)	1.75 (19%)
		$[5^-]$		[2.695(10)]	1.64 (40%)	1.77 (34%)	1.83 (32%)
32	19	1^+	33 ms	1.952(2)	1.83 (6.0%)	1.88 (3.7%)	1.86 (4.7%)
30	17	3^+	3.60 s	3.010(7)	3.00 (0.3%)	3.09 (2.7%)	3.07 (2.0%)
28	15	3^+	2.24 m	3.242(5)	3.08 (5.0%)	3.01 (7.2%)	3.01 (7.2%)

Fig. 2. (Color on-line) (a) Experimental magnetic moments of odd-odd Al isotopes (errors smaller than the dot size) compared to large-scale shell model calculations (data from [11,26]). (b) Calculated contribution of 2p2h configurations in the wave functions.

ground state wave function must be present. To conclude on the exact amount of mixing, a more extended theoretical analysis is needed, which is not the scope of this work.

For the odd-odd Al isotopes the agreement with the calculations is in general somewhat less. That is because these magnetic moments are extremely sensitive to the odd-proton odd-neutron configuration mixing which occurs in these nuclei. Thus these odd-odd moments are a very good test for the validity of the used $sd-pf$ cross shell effective interaction. For the isotopes with $N < 20$, where only the sd shell is supposed to play a major role for protons and neutrons, the agreement between experimental and calculated moments is about 5% or better (Table 1 and Fig. 2a). However, for the $N = 21$ isotope ^{34}Al, which has at least one neutron in the fp shell, both calculations underestimate the magnetic moment by 30% for the 4^- state. The deviation is even larger if we would assume that our measured g-factor corresponds to a 5^- state. This large deviation is a clear signature that in both interactions something is not fully taken into account. In Fig. 2b we compare the predicted amount of $2p2h$ intruder configurations in the odd-odd Al wave functions. Although both models predict a very different amount of intruder mixing in the ^{34}Al 4^- level, they both predict similar values for its magnetic moment. To understand this, we have made constrained shell model calculations with both interactions. The magnetic moments for a pure $(\pi(sd)\nu f_{7/2})_{4^-}$ and $(\pi(sd)\nu p_{3/2})_{4^-}$ configuration are very different, as shown in Fig. 3a. Both interactions predict similar values for these pure configurations, and in a simple two-level mixing calculation it would require more than 70% of $\nu p_{3/2}$ occupation probability to reproduce the experimental 4^- magnetic moment (and thus an inversion of the $\nu f_{7/2}$ and $\nu p_{3/2}$ orbits, which seems most unlikely). A configuration with one neutron in the $p_{3/2}$ orbital can not lead to a spin 5, and thus such mixing can not be considered to explain the deviation between experiment and theory in this case. The effect of intruder components in the 4^- wave function is demonstrated in Fig. 3b, where constrained calculations are made for pure $0p0h$ and $2p2h$ configurations. Both interactions predict a different value for the $0p0h$ configuration. That is because they differ in the $N = 28$ gap: the $0p0h$ magnetic moment is larger with sdpf.sm due to a larger contribution from $\pi(sd)\nu p_{3/2}$ (13% as compared to 6% for SDPF-M), which occurs because the $N = 28$ gap is 500 keV smaller in the sdpf.sm. This does however not affect the conclusion related to the amount of mixing with intruder configurations needed in the wave function, to reproduce the experimental 4^- moment. With both interactions, a simple two-level mixing calculation predicts that between 55% and 70% of intruder configurations is needed to account for the observed large magnetic moment. Inclusion of intruder configurations in the 5^- wave function leads to a magnetic moment that is at most $2.31\mu_N$ for a pure $2p2h$ configuration, which is well below the experimental 5^- value. In conclusion, an agreement between the observed magnetic moment and shell model values using two commonly used interactions in the $sdpf$ shell model, can be obtained for the 4^- state, by considering the subtle interplay between the effect of the reduced $N = 20$ gap (leading to more intruder contribution) and the reduced $N = 28$ gap (leading to more mixing with $\nu p_{3/2}$).
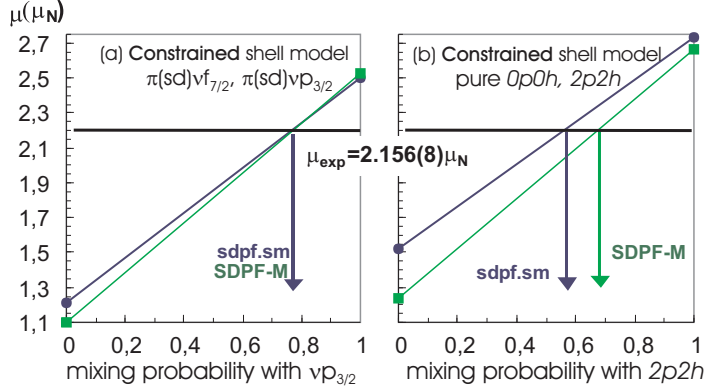
Fig. 3. (a) Linear interpolation between calculations constrained to $(\pi(sd)^5 \nu f_{7/2})_{4-}$ and $(\pi(sd)^5 \nu p_{3/2})_{4-}$ configurations. (b) Same for calculations restricted to pure $0p0h$ and $2p2h$ 4^- configurations.

In an attempt to see the effect of a reduced $N = 28$ gap in SDPF-M, we lowered the single particle energy of the $\nu p_{3/2}$ level by 500 keV in order to reproduce the ^{35}Si $3/2^-$ energy (as it was done before in the sdpf.sm). With this modified SDPF-M' the magnetic moments of the isotopes with $N \leq 20$ are not changed much, because this $\nu p_{3/2}$ level does not play a role in their wave function (see Table 1). However, the magnetic moment for ^{34}Al significantly changes towards the experimental value and the amount of intruder mixing increases as well (triangles in Fig. 2a and 2b). Thus a combination of both effects - a significant mixing with intruder configurations and a significant mixing with $\pi(sd)\nu p_{3/2}$ components - is the key to better agreement with the experimental magnetic moment of this $N = 21$ isotope. This illustrates the importance of dipole moments for probing unknown changes in the effective single particle levels.

It is of importance to test the SDPF-M and SDPF-M' results with other available experimental data on ^{34}Al, shown in Fig. 4. All calculated levels are mixed with intruder $npnh$ configurations ($n = 1, 3$ for positive parity and $n = 2, 4$ for negative parity states). The g factor and the amount of $npnh$ mixing are given for all 4^- and 5^- levels. The modified SDPF-M' (as well as the sdpf.sm) correctly predicts the 4^- as the ground state. This is due to the lower $\nu p_{3/2}$ level, which pushes the 4^- level down relative to the 5^-, because of an increased mixing with $(\pi d_{5/2}^{-1} \nu p_{3/2})_{4-}$ components. The experimental g factor is in-between the value for the 4^- ground state and for the 4_1^- first excited level around 650 keV, both with very mixed normal/intruder configurations. This suggests that the real amount of intruder mixing is somewhere between these values, in agreement with the predictions from the simple two-level mixing calculations.

Only one excited state is known in ^{34}Al, populated through an intermediate energy Coulomb excitation reaction [27] via a highly collective transition

with $B(E2, g.s. \rightarrow ex.) = 100(39)e^2 fm^4$. The B(E2) transition rates to the lowest $(2,3,4)^-$ levels calculated with the SDPF-M' (Fig. 4) with standard effective charges $e_\pi = 1.3e$ and $e_\nu = 0.5e$, show best agreement for populating the second 4_2^- level, thus suggesting that this is the most likely spin/parity assignment to this level.
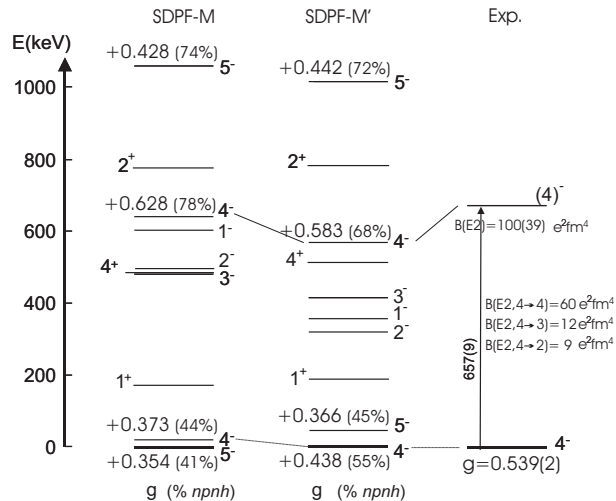

Fig. 4. Levels below 1 MeV calculated with the SDPF-M and SDPF-M' interactions compared to experimental data.

We summarize our qualitative present available knowledge about the island of inversion in Fig. 5. The nuclei for which intruder components are established in their ground state, appear as an island above the 'normal' isotopes. The color scale should be taken as a rough guide as to whether the isotope has a mainly normal dominant (yellow) or intruder dominant (red) ground state. The information for the isotopes in red is taken from [29] for ^{30}Ne, [8] for the Na isotopes, [5] for ^{31}Mg, [30] for ^{32,34}Mg, [31] for ^{33}Mg, [11] for ^{33}Al and this work for ^{34}Al. The Si isotopes are placed outside the island with a question mark for ^{34}Si, based on the work of Baumann et al. [21] and Ibbotson et al. [10]. The other Si isotopes are found in agreement with normal ground state configurations [10,23]. Concerning the ^{33,34}Al isotopes, we concluded that the amount of mixing in the $N = 21$ isotope ^{34}Al is more important than in the $N = 20$ isotope ^{33}Al, by comparing their measured g factors to the existing shell model calculations with free g factors. To investigate this in further detail, other observables such as spectroscopic factors taken from knockout reactions need to be measured and compared to the predictions by different shell model calculations.

Summarizing these results in a qualitative figure, illustrates that a gradual transition from the 'normal' sd-shell region into the island of inversion happens not only as a function of N (as illustrated before in [8]), but also as a function of Z as illustrated by the present data.
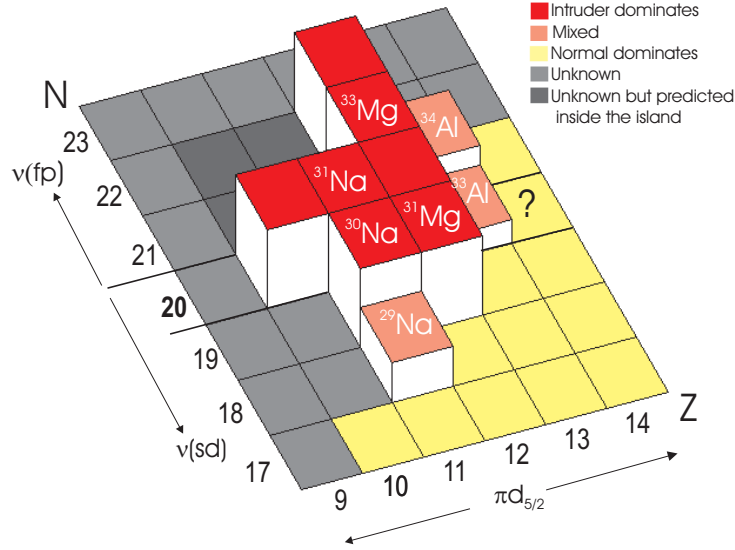
Fig. 5. Isotopes in and near the island of inversion: intruder dominant ground states (red), normal ground states (yellow) and mixed configurations (rose). Isotopes with yet unknown configurations are in light grey and the unknown isotopes from the initially defined island in dark grey.

In conclusion, the ground state structure of an $N = 21$ isotone with a hole in the $\pi d_{5/2}$ orbital could be investigated for the first time. The measured g factor of the ^{34}Al ground state, $|g| = 0.539(4)$, confirms the assigned spin/parity 4^-. The magnetic moment $\mu = (+)2.156(16)\mu_N$ is much larger than the values calculated with the most recent large-scale shell model interactions. This has two causes: the magnetic moment is extremely sensitive to mixing with intruder configurations in the wave function (related to the $N = 20$ shell gap), but also to the occupation of the $\nu 1p_{3/2}$ orbital (related to the $N = 28$ shell gap). Contrary to earlier studies suggesting that Al isotopes have a normal ground state across the $N = 20$ region, this result establishes a large mixing of at least 50% of intruder configurations in the ^{34}Al ground state. Furthermore, the subtle interplay between the effect of reduced $N = 20$ and $N = 28$ shell gaps at $Z = 13$ observed through the g factor, will provide a severe test for a further improved effective shell model interaction. This is indispensable information, that cannot be deduced from binding energies or from decay and level scheme studies.

References

[1] C.Thibault et al., Phys. Rev. **C 12**, 644 (1975).

[2] T. Motobayashi et al., Phys. Lett. **B 346**, 9 (1995).

[3] E. K. Warburton et al., Phys. Rev. **C 41**, 1147 (1990).

[4] M. Keim et al., AIP Conf. Proc **455**, 50 (1998).

[5] G. Neyens et al., Phys. Rev. Lett. **94**, 022501 (2005).

[6] Y. Utsuno et al., Phys. Rev. **C 60**, 054315 (1999).

[7] T. Otsuka et al., Phys. Rev. Lett. **87**, 082502 (2001).

[8] Y. Utsuno et al., Phys. Rev. **C 70**, 044307 (2004).

[9] T. Otsuka et al., Phys. Rev. Lett. **95**, 232502 (2005).

[10] R. W. Ibbotson et al., Phys. Rev. Lett. **80**, 2081 (1998).

[11] P. Himpe et al., Phys. Lett. **B 643**, 257 (2006).

[12] A.C. Morton et al., Phys. Lett. B544, 274 (2002).

[13] S. Nummela et al., Phys. Rev. **C 63**, 044316 (2001).

[14] E. Caurier et al., Eur. Phys. J. **A 15**, 145 (2002)

[15] R. Neugart and G. Neyens, *Nuclear Moments*, in Lect. Notes Phys. **700**, 135 (2006).

[16] D. Borremans et al., Phys. Rev. **C 66**, 054601 (2002).

[17] D.E. Groh et al., Phys. Rev. Letters **90**, 202502 (2003).

[18] K. Turzó et al., Phys. Rev. **C 73**, 044313 (2006).

[19] R. Anne et al., Nucl. Inst. Meth. Phys. Res. **B 70**, 276 (1992).

[20] P.Himpe, Ph.D. Thesis K.U. Leuven, 2006, unpublished.

[21] P. Baumann et al., Phys. Lett. **B 228**, 458 (1989).

[22] V. Paar et al., Nucl. Phys. **A 331**, 16 (1979).

[23] G. Neyens et al., Eur. Phys. J. **A**, (RNB7) in press (2007).

[24] J. Retamosa et al., Phys. Rev. **C 55**, 1266 (1997).

[25] B.H. Wildenthal, Progr. Part. Nucl. Phys. **11**, 5 (1983).

[26] H. Ueno et al., Phys. Lett. **B 615**, 186 (2005).

[27] B.V. Pritychenko et al., Phys. Rev. **C 63**, 047308 (2001).

[28] D. Borremans et al., Phys. Lett. **B 537**, 45 (2002).

[29] Y. Yanagisawa et al., Phys. Lett. **B 566**, 84 (2003).

[30] O. Niedermaier et al., Phys. Rev. Lett. **94**, 172501 (2005).

[31] D.T. Yordanov et al., Phys. Rev. Lett., accepted (2007).

[32] Y. Utsuno et al., Phys. Rev. **C 64**, 0011301(R) (2001).